JOURNAL OF NANO- AND ELECTRONIC PHYSICS
Vol. **6** No 1, 01001(16pp) (2014)

ЖУРНАЛ НАНО- ТА ЕЛЕКТРОННОЇ ФІЗИКИ
Том **6** № 1, 01001(16cc) (2014)

Nanocomposite Apatite-biopolymer Materials and Coatings for Biomedical Applications

L.F. Sukhodub[1,*], G.O. Yanovska[2,†], L.B. Sukhodub[1], V.M. Kuznetsov[2,‡], O.S. Stanislavov[2]

[1] *Sumy State University of Ministry Science and Education of Ukraine, 2, Rymsky-Korsakov St.,40007 Sumy, Ukraine*
[2] *Institute of Applied Physics of National Academy of sciences of Ukraine, 58, Petropavlovska St., 40007 Sumy, Ukraine*

(Received 16 December 2013; published online 06 April 2014)

The microoverview paper describes synthesis and characterization of novel third generation composite biomaterials and coatings which correspond to the second structural level of human bone tissue (HBT) organization obtained at Sumy state university "Bionanocomposite" laboratory. To obtain such composites an animal collagen is usually used, which is not potentially safe for medical applications. That is why investigations were started using some other biopolymers to obtain composites close to the second level in the structural hierarchy of HBT.

Proposed natural polymers (Na alginate, chitosan) are the most perspective because they have bacteriostatic properties for a vast number of aerobic and anaerobic bacteria, high biocompatibility towards the connective tissue, low toxicity, an ability to improve regenerative processes during wounds healing, degradation ability with the creation of chemotaxic activity towards fibroblasts and osteoblasts. The formation of nanosized (25-75 nm) calcium deficient hydroxyapatite (cdHA) particles in the polymer scaffold approaches the derived material to the biogenic bone tissue, which can provide its more effective implantation.

The influence of the imposition of static magnetic field on brushite ($CaHPO_4 \cdot 2H_2O$) crystallization was also investigated. It was shown that changing the magnetic field configuration could greatly affect crystallinity and texture of the derived particles.

To increase the biocompatibility of existing medical implants (Ti–6Al-4V, Ti-Ni, Mg) the technology for obtaining bioactive coatings with corresponding mechanical, structural and morphology characteristics is developed in our laboratory. In this direction coatings based on cdHA in combination with biopolymer matrices (Na alginate, chitosan,) are obtained in "soft" conditions using a thermal substrate technology. This technology was proposed by Japan scientists [1] and was sufficiently improved by us [2] in order to obtain coatings in the controlled mode.

Keywords: Composite biomaterials, Hydroxyapatite, Coatings, Chitosan, Alginate, XRD, XRF, FTIR, SEM, TEM.

PACS numbers: 87.85.J –, 87.64.Bx, 87.64.Ee

1. INTRODUCTION

Human bone tissue (HBT) represents a very complicated composite material with a multilevel structural organization. Collagen fibrils are mineralized by hydroxyapatite (HAp) and that corresponds to the second structural level of HBT organization. In this structure, HAp crystals have the appearance of nanostructured plates with such dimensions: length ~ 50 nm, width ~ 25 nm and thickness ~ 2 nm. HAp is the main mineral of bones, dentin and tooth enamel of human body and usually corresponds to the so-called calcium-deficient HAp (cdHAp) with a carbonate component. To obtain second level composites, scientists usually use an animal collagen, which is not potentially safe for medical applications. Gelatin – a partly hydrolyzed collagen product – also has a disadvantage when it is used as a polymer component in apatite composites: a very high resorption rate compared to the osteogenesis one. That is why investigations were started using some other biopolymers to obtain composites close to the second level in the structural hierarchy of HBT. Such approach, when both natural (Na alginate, chitosan) and synthetic (polyvinyl alcohol, acrylamide) polymers on the one hand and cdHAp on the other are used, is a subject of investigation at Sumy state university "Bionanocomposite" laboratory with a task to obtain some novel biomaterials and coatings for practical medicine. These materials correspond to the third biomaterial generation, which are characterized as osteoconductive (a support of osteoforming cells), as well as osteoinductive (a stimulation of osteosynthesis of new bone de novo) properties. Proposed natural polymers (Na alginate, chitosan) are the most perspective because they have bacteriostatic properties for a vast number of aerobic and anaerobic bacteria, high biocompatibility towards the connective tissue, low toxicity, an ability to improve regenerative processes during wounds healing, degradation ability with the creation of chemotaxic activity towards fibroblasts and osteoblasts. The addition of metal (gold, silver) nanoparticles improves its antibacterial properties. Each component of the prepared nanocomposite will be involved in obtaining the end product with specific properties. So, e.g., due to the formation of nanosize cdHAp particles the structure of the material will be close to the biogenic bone tissue and this will accelerate the formation of the own bone tissue at the implantation place. The presence of metal nanoparticles induce a bacteriostatic effect towards aerobic and anaerobic stems of

* l_sukhodub@yahoo.com
† biophy@yandex.ua
‡ vkuznetsov.ua@gmail.com

microorganisms and a modified polymer matrix will allow to produce a prolonged and controlled release of some necessary chemotherapy compounds (antibiotics, anti-inflammation, anesthetic substances). To increase the biocompatibility of existing medical implants (Ti-6Al–4V, Ti-Ni, Mg) the technology for obtaining bioactive coatings with corresponding mechanical, structural and morphology characteristics is developed in our laboratory. In this direction coatings based on cdHAp with biopolymer matrices (Na alginate, chitosan, gelatin) are obtained in "soft" conditions using a thermal substrate technology. This technology was proposed by Japan scientists [1] and was sufficiently improved by us [2] in order to obtain coatings in the controlled mode.

2. MATERIALS AND METHODS

2.1 Materials Synthesis

2.1.1 Hydroxyapatite and Calcium-Deficient Hydroxyapatite

Hydroxyapatite ($Ca_{10}(PO_4)_6(OH)_2$) was synthesized using commercially obtained analytically grade starting precursors ($Ca(CH_3COO)_2$, NaH_2PO_4, NaOH, $Ca(NO_3)_2{\cdot}4H_2O$, $(NH_4)_2HPO_4$, NH_4OH) by the following chemical reactions (1, 2) respectively:

$$10{\cdot}Ca(CH_3COO)_2 + 6{\cdot}NaH_2PO_4 + 14{\cdot}NaOH = \\ = Ca_{10}(PO4)_6(OH)_2 + 20{\cdot}CH_3COONa + 12{\cdot}H_2O \quad (1)$$

at pH = 11-12 by adding the aqueous solution of 10 M NaOH , heating at 80 °C for 10 min, aging for 12-24 hours, washing by deionized water, sintering at 900 °C for 1 hour,

$$5{\cdot}Ca(NO_3)_2{\cdot}4{\cdot}H_2O + 3{\cdot}(NH_4)_2HPO_4 + 4{\cdot}NH_4OH = \\ = Ca_5(PO_4)_3OH + 10{\cdot}NH_4NO_3 + 23{\cdot}H_2O \quad (2)$$

at pH = 11-12 by by adding the aqueous solution of 25 % NH_4OH, heating at 80 °C for 10 min, aging for 12-24 hours, washing by deionized water, sintering at 900 °C for 1 hour.

One of the important characteristics of HAp is its stoichiometry reflected by Ca / P ratio. For nonstoichiometric HAp such formula is normally used

$$Ca_{10-x}(HPO_4)_x(PO_4)_{6-x}(OH)_{2-x}{\cdot}nH_2O \\ (1.5 < Ca / P < 1.67, \text{ and } 0 < x < 1, n = 0\text{-}2.5)$$

Biological apatite in natural bone contains a considerable amount of carbonate ions (about 7.4 mass % with respect of natural bone) [3]. Carbonate HAp (CO_3^{-}-HAp), which replaces PO_4^{3-} and / or OH^- with CO_3^- ions, is similar to the inorganic component of bone, and may be more perspective material than pure HAp for bone replacement. One of ways used in our work for obtaining such kind of materials is the addition of $NaHCO_3$ to the reaction.

2.1.2 Mg-substituted Brushite under the Influence of a Static Magnetic Field

Calcium phosphate cements based on brushite (dicalcium phosphate dehydrate, DCPD, $CaHPO_4{\cdot}2H_2O$) are widely used due to their high resorbability *in vivo* [4]. Brushite can transform into hydroxyapatite (HAp) [5] in aqueous solutions at 36-37 °C. Solubility and ability of brushite transformation *in vivo* grants certain preferences in its use as a coating for metallic implants. Calcium-phosphate crystallization is affected considerably by different physical conditions, e.g. temperature, pH, ionic strength, presence of different additions and imposition of magnetic field. The DCPD, metastable at room temperature, can be stabilized by the presence of the Mg substrate [6]. The synthesis was carried out at 25 °C with and without the imposition of 0.3 T static magnetic field. Glasses with precursor solutions containing $CaCl_2$ and Na_2HPO_4 with Ca / P = 1.67 were placed on both sides of magnets in proximity to south and north poles (Fig. 1) with each glass containing a single Mg substrate.

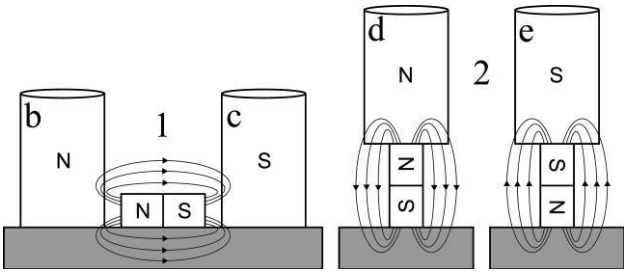

Fig. 1 – Experimental setup showing two magnetic field configurations and samples names

2.1.3 Biphasic Calcium Phosphates

HAp has a low level of solubility ($K_S = 3{\cdot}10^{-116}$) [7]. The transition to the biphasic composites is one of the ways of improvement resorption for materials based on HAp which contain more soluble components, e.g. tricalcium phosphate (TCP) $Ca_3(PO_4)_2$, $K_S = 0.2{\cdot}10^{-29}$ [7]. The biphasic composite containing HAp and TCP was obtained in our studies. The initial components for synthesis were calcium acetate $Ca(CH_3COO)_2$ (0,167 mM), sodium dihydrogen phosphate NaH_2PO_4 (0,1 mM), sodium hydrocarbonate $NaHCO_3$ (0,02 mM). Equal conditions for simultaneous interaction of PO_4^{3-} and CO_3^{2-} ions with Ca^{2+} and OH^- ions were provided by adding mixed solution of NaH_2PO_4 and $NaHCO_3$. The calcium phosphate composite was formed at pH = 11 by drop wise adding of 10 M NaOH aqueous solution at 80 °C. The formed calcium phosphate suspension after aging for 24 hours was carefully washed with deionized water and heated in a muffle furnace at 900 °C for 1 hour. The samples with and without addition of $NaHCO_3$ were synthesized.

2.1.4 Chitosan / Alginate / Hydroxyapatite (CS / ALG / HAp)

For fabrication of CS / ALG / HAp composites the following precursors were used: chitosan (MW 500 kDa, deacytelation degree 80.5 %, "Bioprogress", Moscow), sodium alginate (E401), and analytical grade sodium hydrophosphate (Na_2HPO_4), calcium acetate $(CH_3COOH)_2Ca{\cdot}H_2O$, (China). The cationic-anionic cooperative interaction between CS and ALG macromolecules is a main driving force of their complexation. A biopolymer matrix based on the CS solution (2 g/l in 1 % acetic acid) was prepared with following mixing in a shaker (KS

4000i, 200 rpm, 37 °C) for 1 hour. Then, 1 g of sodium alginate was added to the chitosan solution and mixed for 3 hours. For HAp nucleation on the biopolymers, 0.1 M Na_2HPO_4 (60 ml) and 0.1 M $(CH_3COO)_2Ca \cdot H_2O$ (100 ml) were added to the suspension with adjusting pH to 11 by adding NaOH (18 wt. %). Then, the solution was heated at 80 °C with aging for 48 hours. The obtained product was washed three times by deionized water to pH = 7-7.4. After that, the product was dried at 60 °C and freeze-dried at – 50 °C in 0,4 mBar vacuum for 6 hours. As a result, the 1 : 1 : 1 ratio CS / ALG / HAp composite was obtained.

2.2 Coatings

2.2.1 Common Used Methods

Deposition of bioactive calcium-phosphate coatings on metal substrates provides biocompatibility, chemical inertness and mechanical strength of medical implants. Biocompatibility and bioactivity of biomaterials considerably depend on their surface properties, since chemical reactions occur directly on the surface of implants after implantation into the body [8]. Therefore, surface properties of implants (roughness, porosity, crystallinity, phase composition, morphology, thickness of the coating, chemical purity, microstructure, adhesion) influence the implant interaction with surrounding tissues in the living body. Several techniques are available for the application of HAp coatings onto metal substrates. Plasma spraying is a common commercially accepted technique used for production of orthopedic implants [9-10], thermal spraying [11], magnetron sputtering [12-14], ion beam assisted deposition (IBAD) [15], pulsed laser deposition [16], ion deposition [17], ion implantation [18].

Table 1 – The main advantages and disadvantages of coating deposition methods on metal implants

№	Method	Advantages	Disadvantages	References
1.	Plasma spraying	– commercially accepted; – deposition of coatings with 50-200 μm thickness.	– porous surface of a substrate is needed for deposition; – difficulties in single phase HAp coating formation; – high temperatures of deposition	[9, 10]
2.	Thermal spraying	– low cost; – high efficiency; – coatings have micro-rough surface; – high deposition rates.	– decomposition of HAp at high temperatures; – formation of amorphous coatings and nanostructures due to the fast cooling.	[9, 11]
3.	Ion beam technique	– crack-free coatings deposition with maintaining of surface topography; – excellent adhesion; – the possibility of introduction drugs in coating material.	– high cost of equipment; – high deposition temperatures and possibility of thermal decomposition; – vacuum needed.	[9, 15, 17, 18]
4.	Pulsed laser deposition	– deposition of coatings with 0.05-5 μm thickness and excellent adhesion to the substrate; – coating deposition on various substrates (metals, polymers); – possibility of coating deposition on both sides of implant surface; – control of coating crystallinity and chemical composition.	– high cost; – vacuum needed; – high temperatures cause the oxidation of metal or alloy substrates.	[9, 16]
5.	Sputtering deposition	– dense coatings with uniform thickness on flat surfaces.	– low deposition rate; – high cost	[9, 12-14]
6.	Electro-phoresis	– uniform coating thickness; – high deposition rates; – suitable for substrates with complex shape.	– non uniform thickness; – low bond strength of the coatings; – cracks on the coatings	[9, 21]
7.	Sol-gel	– suitable for substrates with complex shapes; – low processing temperatures.	– expensive raw materials; – organic toxic solvent	[19, 27, 28]
8.	Biomimetic method	– low processing temperature technique; – suitable for substrates with complex shapes.	– time-consuming method; – replacement of solution; – control of solution pH	[9, 25]
9.	Thermal substrate method	– low processing temperature technique; – suitable for substrates with complex shapes; – direct deposition from aqueous solutions on substrate surface; – fast deposition (10-180 min); – coatings with controlled phase composition, morphology and porosity; – coatings with addition of biopolymers, antibacterial components, drugs.	– require changes in experimental setup for coating deposition on substrate with complex shape or various compositions.	[1, 2, 26, 27, 29]

All mentioned methods require high temperatures of coatings deposition. Among low-temperature methods are sol-gel method [19-20], electrophoretic method [21], electrochemical deposition [22-23], hydrothermal deposition [14], electrical sputtering [24]. Any of the mentioned methods has its advantages and disadvantages related to physical-chemical and structural parameters of layers, mechanical properties (Table 1). Biomimetic methods grow increasingly popular for coatings deposition in close to physiological conditions [25]. These methods are widely used for substrates of a complex geometry, but a preliminary treatment of substrates is needed, since untreated substrates have no sufficient bioactivity to form a calcium phosphate coating.

2.2.2 Thermal substrate method

The thermal substrate method (TSM) is an alternative means to form coatings from aqueous solutions [1, 26-28]. In the work [2] this method was considerably improved by adding a cooling system, mixing in solution and glass with reference solution. The TSM allows obtaining calcium-phosphate coatings of various thicknesses on Ti substrates from aqueous solutions with different ion composition. This method has several advantages: 1) coating is formed directly on the substrate surface due to the supersaturation, caused by a local increasing the temperature of substrate. 2) Coatings of various thicknesses are deposited without precipitation in solution. 3) Fast coating formation (up to 0.5 mm in thick during 1 hour of deposition). 4) Deposition of coatings with various phase content, morphology and porosity on substrates with complex geometry. 5) Possibility of introducing biomolecules, biopolymers drugs and antibacterial components into the coatings [1].

The main feature of the thermal substrate method used to form HAp coatings is the thermal activation near the substrate, immersed in aqueous solutions, containing components for hydroxyapatite synthesis. The local increase in the temperature of a substrate and the availability of calcium, phosphate, and hydroxide ions in solution near the substrate accelerate the formation of a HAp coating on the substrate surface. It is known [7], that the solubility of HAp in aqueous solutions decreases with increasing temperature. This is the main principle for TSM. The relationship between the solubility constant of HAp (Ks (mol dm^{-3})[9]) and temperature T(K) is given by following equation [7]:

$$\log Ks = \log[Ca^{2+}]^5[PO_4^{3-}]^3[OH^-] = \\ = \frac{-8219.41}{T} - 1.6657 - 0.098215T. \quad (3)$$

Rate of coating deposition depends on a substrate temperature, surface roughness, pH of the initial solution, ion concentrations, ion composition, deposition time [26-27]. Rate of coating deposition depends on a substrate temperature, surface roughness, pH of the initial solution, ion concentrations, ion composition, deposition time [26-27]. The experimental setup is proposed for calcium-phosphate coating deposition by TSM (Fig. 2).

The experimental setup consists of two glasses that immersed in general container equipped with cooling system. One of them is for experimental solution (initial solution) and another one – for distilled water (reference solution). The glass with distilled water was added for controlling substrate temperature in solution. Substrates made of Ti or Ti-6Al-4V alloy were used for coatings deposition. They were attached to the copper electrodes by stainless steel bolts and immersed in the solutions. One of the substrates was immersed into the aqueous solution containing components for hydroxyapatite synthesis (initial solution) and another one – in reference solution. The temperature of the substrates is measured using a calibrated thermocouple, which is in close contact with the upper surface of the substrate immersed in distilled water for precise temperature measurements. An alternating current (10-40 A) is passed through the substrates via the copper electrodes, which resulted in localized heating of the samples.

The substrate temperature is varied by changing of applied current. Magnetic stirrer is used for mixing in the experimental and reference solutions. Morphology of coatings strongly depends on mixing in the initial solution. We suppose that stirring ensures uniform coatings deposition on substrates.

Cooling system is used for maintaining temperature gradient between hot substrate surface and cool aqueous solution. It is important to control of ion concentrations and pH in the initial solution, substrate temperature should also been controlled because this factors affect the degree of supersaturation near substrate surface. Solution pH is adjusted by adding drop by drop NaOH or NH_4OH solutions. Variation of deposition time allows obtaining coatings with various thicknesses. By controlling of such parameters as ionic composition, ion concentration, pH of the initial solution, substrate temperature, heating time, surface roughness coatings with various characteristics should be obtained.

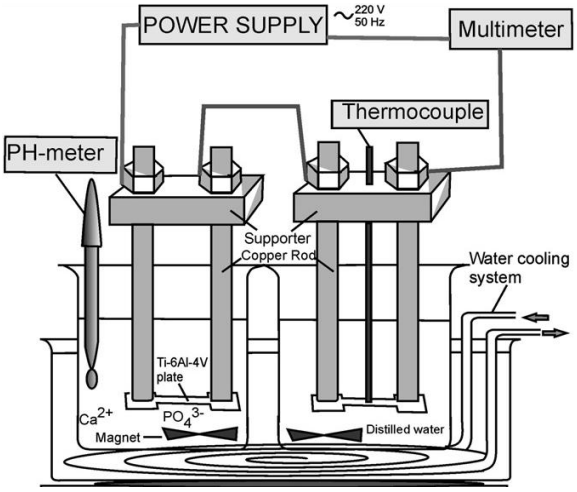

Fig. 2 – Experimental setup for calcium-phosphate coating deposition

2.3 Materials and Coatings Characterization

2.3.1 X-Ray Diffraction Analysis

The crystallinity and microstructure of the synthesized samples were examined using an X-Ray diffractometer DRON-3M (Bourevestnik, Inc., Saint-Petersburg, Russian Federation) connected to a

computer-aided system for the experiment control and data processing. The current and the voltage of the X-ray tube were 20 mA and 40 kV respectively. All experimental data was processed by means of the program package DIFWIN-1 (Etalon PTC, Ltd., Moscow, Russian Federation). Phase identification was performed using a JCPDS card catalog (Joint Committee on Powder Diffraction Standards).

The crystallite sizes L were calculated using the Scherrer equation [30]:

$$L = K\lambda/\beta\cos\theta, \quad (4)$$

where K is the form coefficient (assuming $K = 1$ in our case), λ is the wavelength, β is the peak broadening, θ is the diffraction angle.

The quantitative phase analysis was performed using the reference intensity ratio (RIR) method [31]:

$$C_i = \left(\frac{K_i I_i^{rel}}{I_i} \sum_{i=1}^{n} \frac{I_i}{K_i I_i^{rel}} \right)^{-1}, \quad (5)$$

where C_i is the concentration of the i-phase, K_i is the corundum number of the i-phase, I_i is the chosen peak integral intensity of the i-phase, I_i^{rel} is the peak relative intensity of the i-phase.

The Ca / P ratio was calculated using method described in [32]:

$$\frac{Ca}{P} = \frac{10 \cdot (100 - C_{TCP}) / M_{HAp} + 3 \cdot C_{TCP} / M_{HAp}}{6 \cdot (100 - C_{TCP}) / M_{HAp} + 2 \cdot C_{TCP} / M_{HAp}}, \quad (7)$$

where C_{TCP} is the TCP phase concentration (%), M_{HAp} is the HAp molar mass.

2.3.2 Scanning Electron Microscopy

The surface morphology was examined by scanning electron microscopy (SEM). These investigations were performed in combination with X-Ray emission spectroscopy using the REMMA-102 device (SELMI, Sumy, Ukraine). The surface chemical composition was determined with an energy dispersive X-Ray (EDX) detector. The analytical signal of the characteristic X-Ray emission was integrated by scanning the 50×50 μm^2 area of the sample surface.

2.3.3 Transmission Electron Microscopy

Electron microscopic and electron diffraction studies were conducted after the samples ultrasonic dispersion using the transmission electronic microscope PEM-125K (SELMI PTC, Sumy, Ukraine) with the 90 kV accelerating voltage and the 100 μA beam current. The aperture diaphragm width was 0.1 mm in the electron diffraction mode, the intermediate lenses worked without the magnification. The measurement of the magnetite linear crystallite particle sizes and the results statistical analysis were performed using the VideoTesTRazmer 5.0 program (VideoTesT, Ltd., Saint-Petersburg, Russian Federation). The references to the JCPDS card catalog are supplied when interpreting the electron diffraction patterns.

2.3.4 FTIR Analysis

The Fourier transform infrared spectroscopy studies (Thermo Nicolet Nexus 470 ESP, Minsk Technological University, Belarus) were performed to determine the various functional groups in obtained apatite-biopolymer composites and coatings in 400-5000 cm^{-1} spectral range and 0.125 cm^{-1} resolution. The synthesized powders were ground in an agate mortar and mixed with KBr in 1 : 200 ratio. Transparent pellets were prepared in a stainless form with necessary pressure applied.

2.3.5 X-ray Fluorescent Analysis

ElvaX Light SDD is a desktop energy-dispersive X-ray fluorescence analyzer with extended element range from Na ($Z = 11$) to U ($Z = 92$). It was used for quantitative and qualitative analysis of the elemental composition of synthesized samples. The accuracy of concentrations determination was better than 0.3 %. Analyzer detecting limit was better than 1 ppm for most elements in the light matrix.

2.3.6 *In vitro* (SBF) Analysis

For preparation of the solution, which mineral composition similar to the inorganic component of blood plasma, analytical grade components 7.996 g of NaCl; 0.350 g of $NaHCO_3$; 0.224 g of KCl; 0.228 g of $K_2HPO_4 \cdot 3H_2O$; 0,305 g of $MgCl_2 \cdot 6H_2O$; 40 ml of HCl with 1 kmol/m^3 concentration; 0.278 g of $CaCl_2$; 0.071 g of Na_2SO_4; 6.057 g were sequentially dissolved in 200 ml of distilled water. Tris(hydroxymetil)amino-methane was added for maintaining pH = 7.25, followed by addition of distilled water up to 1 liter. For correction of pH of the HCl solution with concentration of 1 kmol/m^3 HCl could be dropwise added.

3. RESULTS AND DISCUSSION

3.1 Hydroxyapatite and Calcium Deficient Hydroxyapatite

It is important to note that in the case of obtaining pure HAp all secondary products are removed by deionized water.

But when these reactions are used for HAp synchronic obtainment in combination with biopolymers or other molecules removing the secondary products will be more difficult.

Therefore, as an alternative, the reaction (1) with participation of $Ca(CH_3COO)_2$ component was used. In this case, besides HAp, nontoxic CH_3COONa salt is formed which can be easily removed from the organism. X-Ray diffraction analysis of obtained powders heat treated at 600 °C for 1 hour shows that the main phase resulting from reactions (1) and (2) (samples 1, 2) is an amorphous nanocrystalline HAp (Fig. 3).

Further heat treatment leads to the appearance of an additional phase of TCP with its larger amount in the sample 1 (Fig. 3). Phase concentrations and Ca / P ratios for both samples heat treated at 900 °C for 1 hour are shown in Table 2.

The organic component of the mother solution in the reaction (1) influences crystallite sizes: X-ray diffraction patterns for both samples heat treated at

600 °C show the formation of nanocrystalline product, but the average crystallite size for sample 1 is 25.7 nm and for sample 2-35.5 nm. Further heating at 900 °C leads to the increase of average crystallite sizes of both samples making it practically the same (~ 50 nm). Influence of the solution content and the heat treatment on crystallite sizes is shown in Table 3.

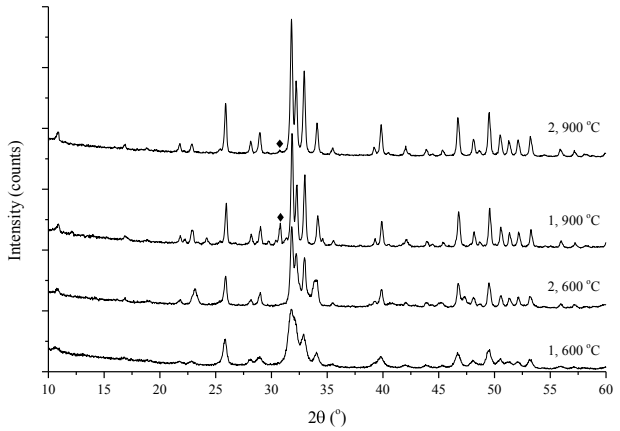

Fig. 3 – XRD patterns for samples 1, 2. TCP main peaks are marked with ♦

Table 2 – Phase composition for samples 1, 2

Sample	HAp		TCP		Ca / P, at. %
	Card	Concentration, %	Card	Concentration, %	
1. T = 900 °C	84-1998	90	9-348	10	1.661
2. T = 900 °C	84-1998	95	9-348	5	1.664

Table 3 – Average crystallite sizes for samples 1, 2

Sample	Phase	Miller indices	L, nm
Synthesis a); 1, T = 600 °C (with organics)	HAp	(0 0 2)	23
	HAp	(0 0 4)	28.5
Synthesis a), 1, T = 900 °C (with organics)	TCP	(1 1 1)	40
	TCP	(1 3 2)	37
	TCP	(4 0 2)	48.3
	HAp	(1 2 1)	45
	HAp	(0 0 4)	56.7
Synthesis b); 2, T = 600 °C	HAp	(0 0 2)	33
	HAp	(0 0 4)	38
Synthesis b); 2, T = 900 °C	HAp	(0 0 2)	45.7
	TCP	(1 7 0)	72.3
	HAp	(1 2 1)	43
	HAp	(0 0 4)	60

Carbonate-apatite samples have been obtained using both base reactions (1, 2) with the addition of 0.2 mM $NaHCO_3$ salt to the mother solution. XRD patterns for samples 5, 7 (reaction 1) and 4, 6 (reaction 2) are shown in Fig. 4.

XRD patterns for samples 4-7 obtained via the reactions (1, 2) and heated at 600 °C show that the crystalinity of the product decreases, in comparison with the samples 1, 2 (Fig. 3), after the addition of Na hydrocarbonate. The further heating at 900 °C increases crystallite sizes with a single feature: crystallites in (1 2 1) plane have bigger sizes obtained via the reaction (1) (50 nm compared to 41 nm of the reaction (2)). The influence of various synthesis methods on crystallite sizes is shown in Table 4. After heating at 900 °C for 1 hour, additional phases in samples 5 and 7, obtained from the solution with the organic component, were observed: calcite and a significant amount of TCP (~ 35 % to total).

The formation of the significant portion of TCP phase in these samples after the heat treatment indicates that the crystallization of non-stoichiometric hydroxyapatite has occurred under the influence of the organic component, and also shows the presence of the defects in the crystal lattice due the partial substitution of Ca^{2+} ions with close in size Na^+ ions (0.99 Å and 0.98 Å respectively) which are presented in the solution.

Additional local defects in the crystal lattice could have been induced by the incorporation of carbonate ions (CO_3^{2-}) which affect the biological behavior of the resulting product increasing its resorption degree [33]. Phase concentrations and Ca / P ratios of samples 4-7 heated at 900 °C are shown in the Table 4.

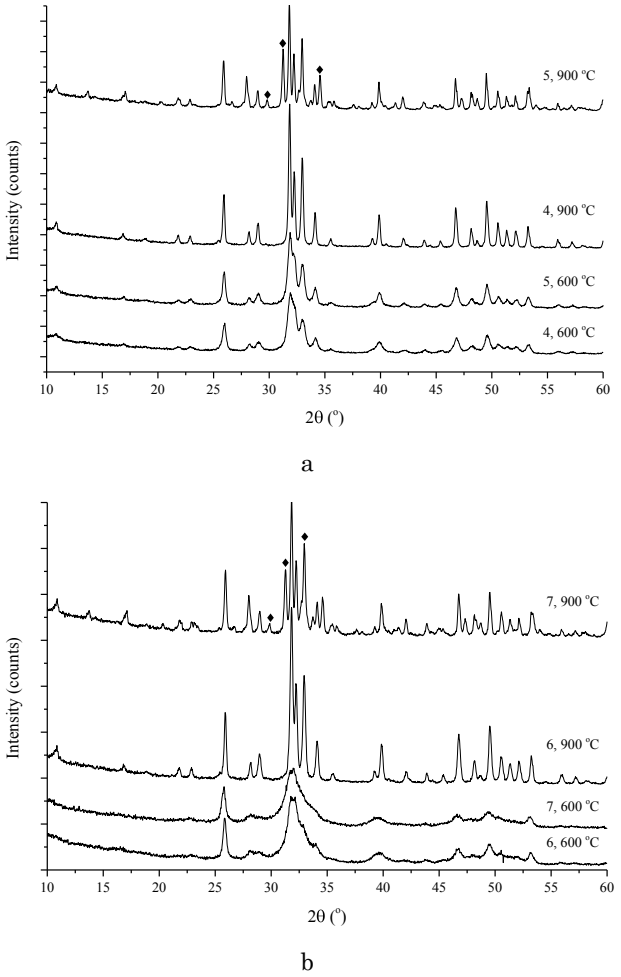

Fig. 4 – XRD patterns for samples 4, 5 (a) and 6, 7 (b). Main TCP peaks are marked with ♦

Table 4 – Average crystallite sizes for samples 4-7

Sample	Phase	Miller indices	L, nm
Synthesis b) , 4, T = 900 °C	HAp	(0 0 2)	45.5
	HAp	(1 2 1)	46.6
	HAp	(0 0 4)	62
Synthesis a), 5, T = 900 °C (with organics)	TCP	(1 0 4)	43.4
	TCP	(3 0 0)	48
	TCP	(0 2 10)	53.4
	HAp	(1 2 1)	53.2
	TCP	(2 2 0)	56.3
Synthesis b) , 6, T = 900 °C	HAp	(0 0 2)	43
	HAp	(1 2 1)	36
	HAp	(0 0 4)	54.7
Synthesis a), 7, T = 900 °C (with organics)	TCP	(1 0 4)	29
	TCP	(3 0 0)	47
	TCP	(0 2 10)	42.5
	HAp	(1 2 1)	48.2
	TCP	(2 2 0)	46.4

3.2 Mg-substituted Brushite Under Influence of Static Magnetic Field

The analysis of the precipitate obtained from the solution with 1.67 Ca / P ratio with and without the imposition of magnetic field in the presence of Mg substrate after two days of precipitation shows the occurrence of a single phase – brushite (JCPDS 72-713). The crystallinity of b- and c- samples of the first magnetic field configuration (1C) remains comparable to the sample, precipitated without the imposition of magnetic field (a-sample), with the crystallinity of the b-sample slightly better than the c- one (Fig. 5).

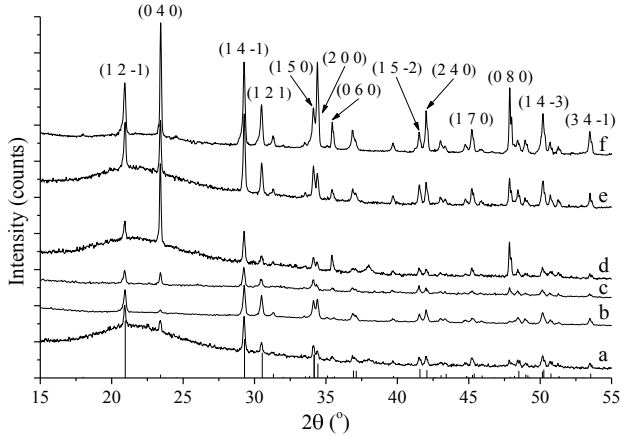

Fig. 5 – XRD patterns for samples with and without the imposition of magnetic field in the presence of Mg and without it (f)

In case of the second magnetic field configuration (2C) the crystallinity perceptibly increases compared to the a-sample. The d-sample has much higher intensities of (0 4 0) and (0 8 0) peaks which means that it is oriented along the b-axis. The mean crystallite sizes (Table 5) of the 2C in most cases are higher than the 1C ones. The crystallite sizes of the a-sample and 2C samples differ insignificantly with the visible distinction in their crystallinity which can be explained by the presence of lattice strains in the a-sample.

Table 5 – Average crystallite sizes in nm for samples a-e

Sample	Miller indices					
	(1 2 -1)	(0 4 0)	(1 2 1)	(1 5 0)	(2 0 0)	(0 8 0)
a	70	55,6	58,8	66	71,3	112
b	52	65,4	53,5	54,8	60,6	83
c	51	81,5	53,7	50	112,6	84,6
d	64,2	96,6	55	61,5	84,2	113,5
e	63,4	78	73,7	67,7	77,2	97,6

It was verified [34] that the Mg substrate availability decreases the crystallinity of DCPD (Fig. 5a and 5f).

The micrographs of the nanoparticles with the different magnifications were obtained by the TEM (Fig. 6). The particle sizes are: a-sample – 50-60 nm, b-sample – 40-80 nm, c-sample – 30-60 nm.

The comparative analysis of the electron microscopy data correlates with the XRD data. The higher sizes of the particles in case of the b-sample can be explained due to the differences between the crystallite and particle sizes thus considering that in this case the particles consist of two or more crystallites.

3.3 Chitosan / Alginate / Hydroxyapatite (CS / ALG / HAp)

Biopolymer-apatite composites are the most perspective materials for tissue engineering because they are close to the 2D structural level in bone structural hierarchy. Instead of animal collagen some other biopolymers as an organic component are used in the synthesis such materials. For example, the composites based on CS and HAp are widely used in clinical applications. Chitosan is a derivative of chitin, a second, after collagen, most abundant natural biopolymer. It is found in shells of marine crustaceans and cell walls of fungi. Structurally, CS is a linear polysaccharide, composed of glucosamine and N-acetyl glucosamine linked in a β(1-4) manner with a molecular weight in the range 300-1000 kDa and degree of deacetylation from 30 % to 95 %.

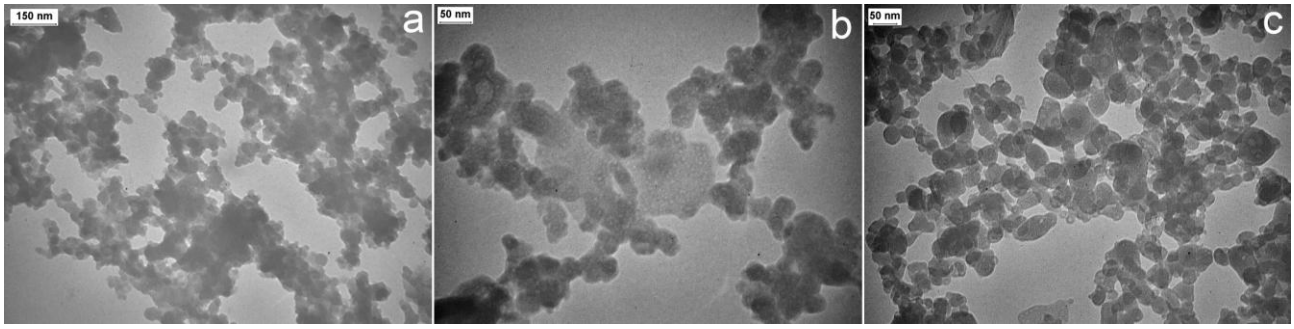

Fig. 6 – Micrographs of the nanoparticles with the different magnifications of a-, b- and c- samples

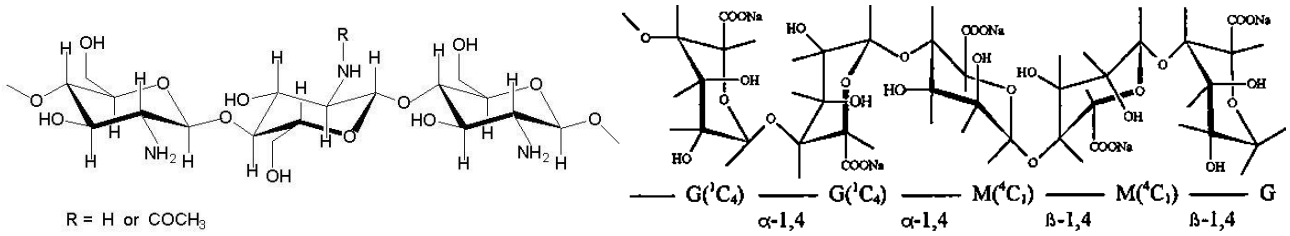

Fig. 7 – Chemical structure of chitosan (left) and sodium alginate (right)

CS interacts electrostatically with negatively charged molecules due the presence of cationic amino groups (Fig. 7). This property is very important because a large number of cytokines / growth factors are bounded to anionic glycosaminoglycans. CS can be molded in various forms and possesses ability to form porous structure by freezing-lyophilizing procedure. Also, CS is characterized its intrinsic antibacterial activity due interactions its amino groups with anions on the bacterial cell walls, suppressing biosynthesis. The second natural polymer suitable for tissue engineering scaffolds is sodium alginate. ALG is an unbranched binary β-D-mannuronic acid (M) and its C-5 epimer α-L-guluronic acid (G) (Fig. 7).

ALG with bivalent ions like Ca^{2+} form insoluble hydrogels. Calcium cross-linked ALG hydrogels have been used in biomedical applications.

Fig. 8 shows the FTIR spectra of composite components (ALG, CS, HAp) and ALG / CS / HAp composite scaffolds with various polymer-apatite ratios. FTIR spectra of ALG scaffold showed an intense peak around 3427 cm^{-1} indicates the absorption of OH group. A peak around 1400-1440 cm^{-1} is due the presence of carboxyl (COOH) group. A peak around 1621 cm^{-1} indicates the presence of carbonyl (CO) group. Peaks at 1000-1132 cm^{-1} region confirmed the presence of guluronic acid, mannuronic acid, the building blocks of alginate (Razy et al., 2002). The chitosan FTIR spectrum showed characteristic bands of amide (around 1600 cm^{-1}), amino (around 1160 cm^{-1}), and C-O stretching (around 1420 cm^{-1}).

FTIR of HAp shows characteristic absorption bands at 3427 cm^{-1}, 1048-1090 cm^{-1}, 576-630 cm^{-1} that are attributed to the O-H stretching mode, triply degenerated asymmetric stretching modes and triply degenerated bending modes of the O-P-O bonds of the phosphate group. For CS / ALG / HAp scaffold, characteristic band which is assigned to amide group appeared at 1584 cm^{-1} ($\Delta = 14$ cm^{-1}), while a peak at 1157 cm^{-1} which is assigned to amino group was observed with very decreased intensity (a big part of amino groups were protonated). From this follows that protonated amines on CS molecules and Ca^{2+} ions of HAp interacted with carboxyl groups on alginate molecules. The SEM investigations the same samples are shown in Fig. 9.

3.4 Hydroxyapatite, Apatite-biopolymer Coatings Formed on Ti and its Alloys Substrates

Table 6 demonstrates experimental conditions and main characteristics of deposited calcium-phosphate coatings obtained by thermal substrate method at our laboratory "Bionanocomposite" and Kuroda's group.

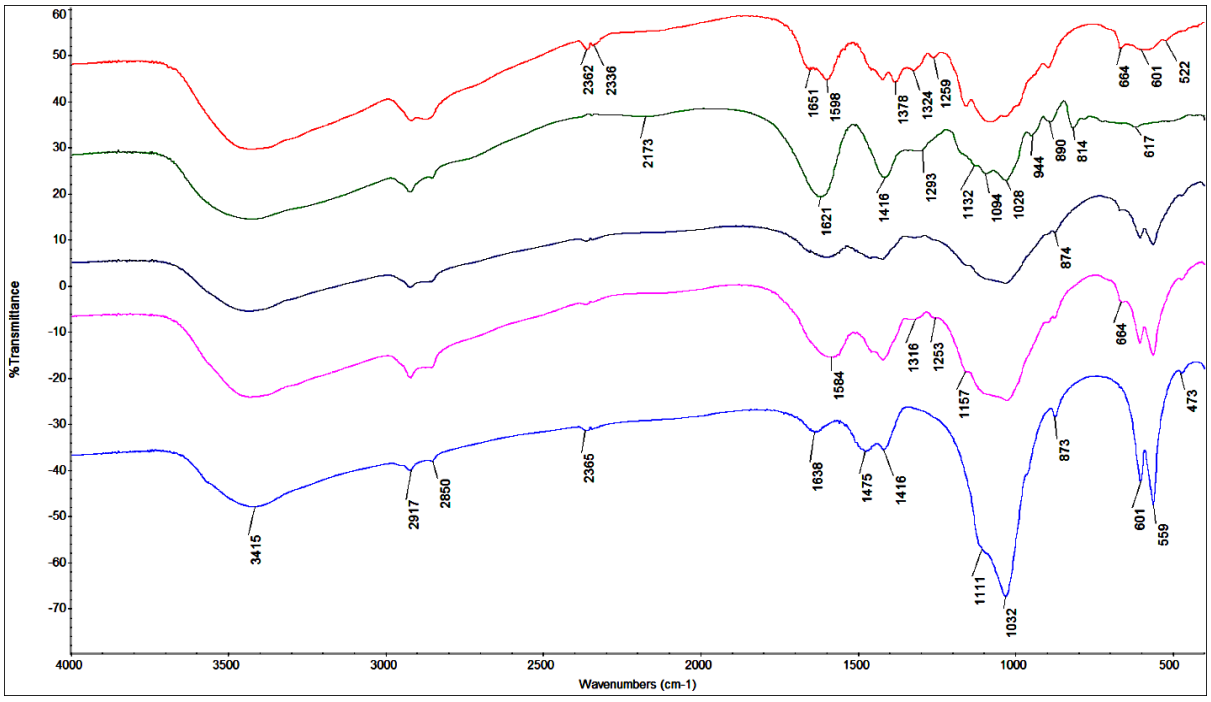

Fig. 8 – FTIR spectra of composite components (ALG, CS) and ALG / CS / HAp composites with different polymer / apatite ratios (top-down – CS, ALG, composites)

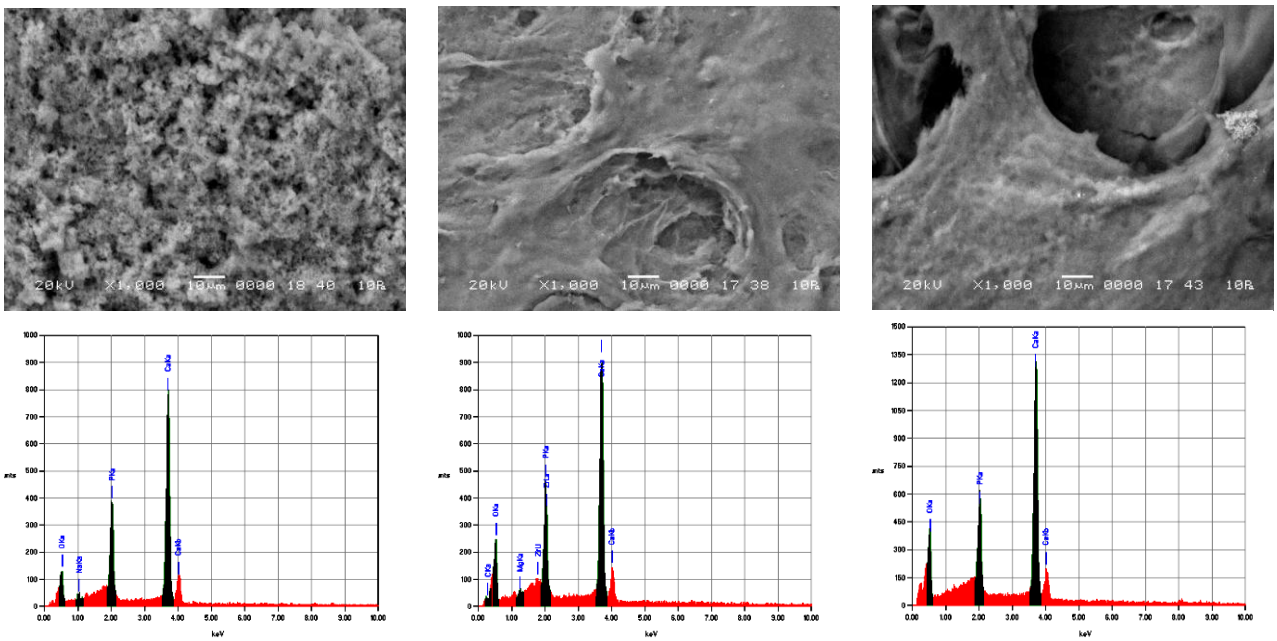

Fig. 9 – SEM micrographs of ALG / CS / HAp and dispersive spectra composites with various polymer/apatite ratios

When the solution pH was less than 5, the main product was monetite (DCPA), with a molar ratio Ca / P = 1.1.

When the pH > 6, HAp was precipitated as a thin plate consisting of tiny needles. The Ca / P ratio of the HAp film was determined to be 1.45, which agrees with values reported for the calcium-deficient apatite formed by electrochemical processes. Hydroxyapatite coating was not formed at pH 8 because ion concentrations were decreased by HAp precipitation in the solution before running the experiment. No precipitates were observed in the solution when the pH was less than 7. Thus, a HAp film can be obtained on the thermal substrate most effectively at neutral pH under appropriate temperature [1].

Carbonate HAp coatings. Coatings deposited from the solution with > 0.5 mM $NaHCO_3$ contained carbonate apatite and calcium carbonate at all temperatures, and the X-ray diffraction spectra showed a mixture of calcite, vaterite, and aragonite, as nature forms of $CaCO_3$ [39].

The crystalline form of carbonate apatite was changed, depending on the added $NaHCO_3$ content, as well as coating temperature. In particular, adding a significant amount of $NaHCO_3$ (> 5 mM) brought about sphere-like carbonate apatite (Type B) in the coating obtained at 140 °C, which was similar to biological apatite. By adding more CO_3^{2-} to the solution the substitution for OH^- (Type A) was obtained. Therefore, in the samples with < 0.5 mM $NaHCO_3$ added, carbonate apatite (Type B) type was obtained, and in the samples with > 5 mM $NaHCO_3$ added, carbonate apatite (Type AB) was formed [39]. Coatings of various phase composition (HAp, DCPD, DCPA, carbonate apatite), biphasic or multiphase coatings with pore size 250-200 μm and required thickness were obtained by thermal substrate method. Crystallinity of the received coatings may also vary greatly. It decreases with decreasing of substrate temperature and in the presence of organic components, like chitosan [29].

Optimal parameters. In the work [36] the optimal parameters were defined: deposition time (at least 60 min), solution pH (6.5) and substrate temperature (100-115 °C). When all required parameters are kept, the coatings with thickness of 50-100 μm may be received with Ca / P ratio close to that in stoichiometric hydroxyapatite (1.67 at. %) (Fig. 10). A vital part of the experiment is the pretreatment and cleaning of the substrate surface with a view to improve the bioactivity and crystallization of HAp. The surface modification prior to the formation of the HAp coating offers the advantage of improving the adhesion strength of the coating to the substrate as well as promoting the bone growth around the HAp-coated implants *in vivo* [29]. Thermal substrate method applied for coatings deposition on complex-shape substrates with various compositions. Titanium and its alloys are widely used as implant materials in dentistry and orthopedic. The Ti-6Al-4V alloy substrates, 36 × 1.9 × 0.36 mm in size, were used for coating deposition [29] (Fig. 10).

They were polished with SiC papers from P100 to P800 grit, washed in acetone (15 min), 96 % ethanol (15 min) and rinsed three times with distilled water under ultrasound treatment.

Chemical surface modification. Some authors [40-49] have reported that surface modifications by soaking in NaOH [41, 42], H_2O_2 [43, 44], acid etching [45] or combination of these methods [44] improve adhesion strength of hydroxyapatite coating to the substrate surface. After soaking in an alkaline solution (e.g. 5 M NaOH at 60 °C for 24 hours), a hydrated titanium oxide gel layer containing Na^+ ions is formed on the surface. Further heating (1 hour at 600 °C) is held for dehydration and solidification of TiO_2 layer and its transformation into sodium titanate with porous net-like structure [42-47]. It becomes a precursor for amorphous calcium phosphate formation with its further transformation to HAp. It is suggested that a porous network of the titanium surface arising after the NaOH pretreatment favors the

Table 6 – Experimental conditions and main characteristics for thermal substrate coating

Temperature, °C	Solution pH	Time of deposition, min	Solution composition, concentrations in mmol/l	Phase composition	Reference
40	8.0	30	0.3 $Ca(H_2PO_4)_2$ 0.7 $CaCl_2$ 1 ethanol ultrasonic treatment	net-like $Ca_{10}(PO_4)_6(OH)_2$	[35]
45	6.5	15	3 $Ca(H_2PO_4)_2$ 7 $CaCl_2$	mainly $CaHPO_4$	[1]
60	8.0	30	0.3 $Ca(H_2PO_4)_2$ 0.7 $CaCl_2$ 1 ethanol ultrasonic treatment	plate-like $Ca_{10}(PO_4)_6(OH)_2$	[35]
75	6.6	120 min	6 NaH_2PO_4 10 $CaCl_2$	amorphous $Ca_{10}(PO_4)_6(OH)_2$	[36]
80	6.7	120 min	6 NaH_2PO_4 10 $CaCl_2$	amorphous $Ca_{10}(PO_4)_6(OH)_2$	[36]
85	6.6	150 min	6 NaH_2PO_4 10 $CaCl_2$	$Ca_{10}(PO_4)_6(OH)_2$	[36]
90	6.6	150 min	6 NaH_2PO_4 10 $CaCl_2$	$Ca_{10}(PO_4)_6(OH)_2$	[36]
95	6.6	120 min	6 NaH_2PO_4 10 $CaCl_2$	$Ca_{10}(PO_4)_6(OH)_2$	[36]
95	6.5	15 min	3 $Ca(H_2PO_4)_2$ 7 $CaCl_2$	$CaHPO_4$ and traces of $Ca_{10}(PO_4)_6(OH)_2$	[1]
100	6.5	120 min	6 NaH_2PO_4 10 $CaCl_2$	$Ca_{10}(PO_4)_6(OH)_2$	[36]
100	7.0	15 min	3 $Ca(H_2PO_4)_2$ 7 $CaCl_2$	$Ca_{10}(PO_4)_6(OH)_2$	[37]
105	6.5	180 min	6 NaH_2PO_4 10 $CaCl_2$	$Ca_{10}(PO_4)_6(OH)_2$	[36]
110	6.6	120 min	6 NaH_2PO_4 10 $CaCl_2$	$Ca_{10}(PO_4)_6(OH)_2$	[36]
115	6.5	120 min	6 NaH_2PO_4 10 $CaCl_2$	$Ca_{10}(PO_4)_6(OH)_2$	[36]
120	6.5	120 min	6 NaH_2PO_4 10 $CaCl_2$	$Ca_{10}(PO_4)_6(OH)_2$	[36]
120	8.0	5 min	3 $Ca(H_2PO_4)_2$ 7 $CaCl_2$	$Ca_{10}(PO_4)_6(OH)_2$	[37]
140	4.0	15 min	3 $Ca(H_2PO_4)_2$ 7 $CaCl_2$	$CaHPO_4$	[1]
140	5.0	15 min	3 $Ca(H_2PO_4)_2$ 7 $CaCl_2$	$CaHPO_4$, amorphous $Ca_{10}(PO_4)_6(OH)_2$	[1]
140	6.0	15 min	3 $Ca(H_2PO_4)_2$ 7 $CaCl_2$	$CaHPO_4$ $Ca10(PO_4)_6(OH)_2$	[1]
140	6.5	15 min	3 $Ca(H_2PO_4)_2$ 7 $CaCl_2$	$CaHPO_4$ $Ca_{10}(PO_4)_6(OH)_2$	[1]
140	7.0	15 min	3 $Ca(H_2PO_4)_2$ 7 $CaCl_2$	$Ca_{10}(PO_4)_6(OH)_2$ with little amount of $CaHPO_4$	[1]
140	8.0	15 min	3 $Ca(H_2PO_4)_2$ 7 $CaCl_2$	mainly $Ca_{10}(PO_4)_6(OH)_2$ with low crystallinity	[1]
140	8.0	15 min	0.3 $Ca(H_2PO_4)_2$ 0.7 $CaCl_2$	needle-like $Ca_{10}(PO_4)_6(OH)_2$	[35]
150	5.0	20 min	3 $Ca(H_2PO_4)_2$ 7 $CaCl_2$	Bricks $CaHPO_4$	[38]
150	6.0	20 min	3 $Ca(H_2PO_4)_2$ 7 $CaCl_2$	thin, plate-like crystals of $Ca_{10}(PO_4)_6(OH)_2$	[38]

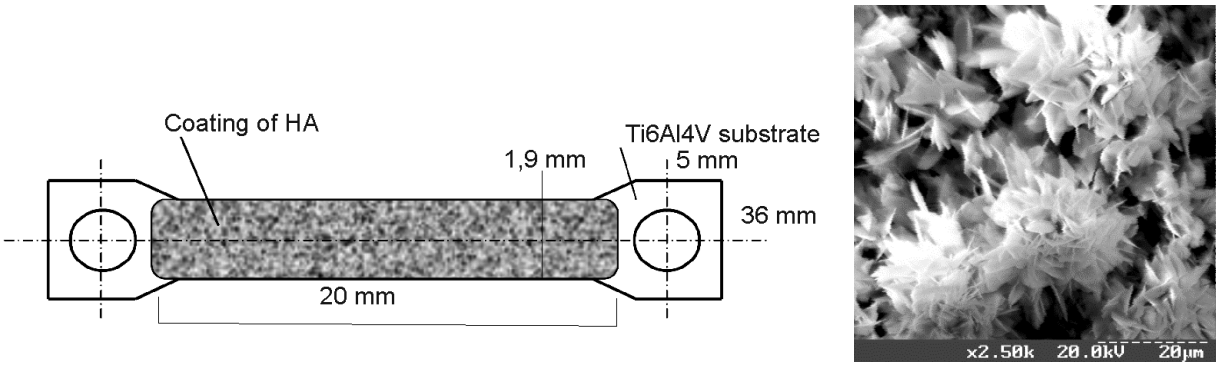

Fig. 10 – Dog-bone shaped model Ti-6Al-4V substrates with deposited coating. Copied from [29] with permission of Elsevier

nucleation of calcium phosphates. The chemical treatment of itanium substrates with an H_2O_2 aqueous solution results in porous TiO_2 layer, with thickness up to 0.06 μm, formed on the Ti surface. The TiO_2, react with hydroxyl ions in the aqueous media, leading to formation of functional Ti–OH groups. In [29] the pretreatment was carried as follows: the cleaned and polished titanium alloy plates were soaked in 200 ml of 35 % NaOH aqueous solution and kept at 60 °C for 2 hours and then for 48 hours at room temperature. The samples were first soaked with a NaOH solution, then thoroughly rinsed with distilled water and finally dried in air at room temperature for 24 h. The H_2O_2-treated substrates were prepared by immersing the titanium alloy substrates in 200 ml of a 35 % H_2O_2 solution and keeping them at 60 °C for 2 hours and then for 48 hours at room temperature. After the H_2O_2 treatment, substrates were thoroughly washed in distilled water and dried in air at room temperature for 24 hours. To obtain a negatively charged surface we used etching (1 min) in a 10 % aqueous solution of HF. The negatively charged surface can significantly increase the rate of the Ca^{2+} ions precipitation from the aqueous solution during the thermal deposition. The acid treated samples were thoroughly rinsed with distilled water and dried in air as described above. Subsequent to the alkali, peroxide and acid treatments the titanium samples were immersed in 200 ml of a solution, containing 10 mmol dm^{-3} $CaCl_2$ and 6 mmol dm^{-3} Na_2HPO_4 to produce bone like apatite on thermally activated titanium surfaces at solution pH = 6.5, substrate temperature 105 °C, 2-hour treatment [29].

Porous coatings. The porous coatings have been obtained on substrates modified by immersion into NaOH, H_2O_2 and HF solutions (Fig. 11-13) [29]. Chemical pretreatment of substrates prior to deposition of calcium-phosphate coatings increases the rate of their formation. It is connected with increasing of crystal nucleation on the surface of modified substrates. The negative-charged groups like $-OH^-$, $-F^-$ initiate nucleation. Furthermore, the acid etching increases surface roughness and that also activate nucleation sites. The alkali treatment was carried out at 60 °C ± 1 °C for 2 hours and continued at room temperature for 48 hours.

The HAp coating was deposited by thermal substrate method under following conditions: substrate temperature of 105 °C, solution pH = 6.5, 2-hour treatment. We suppose that after NaOH-treatment of

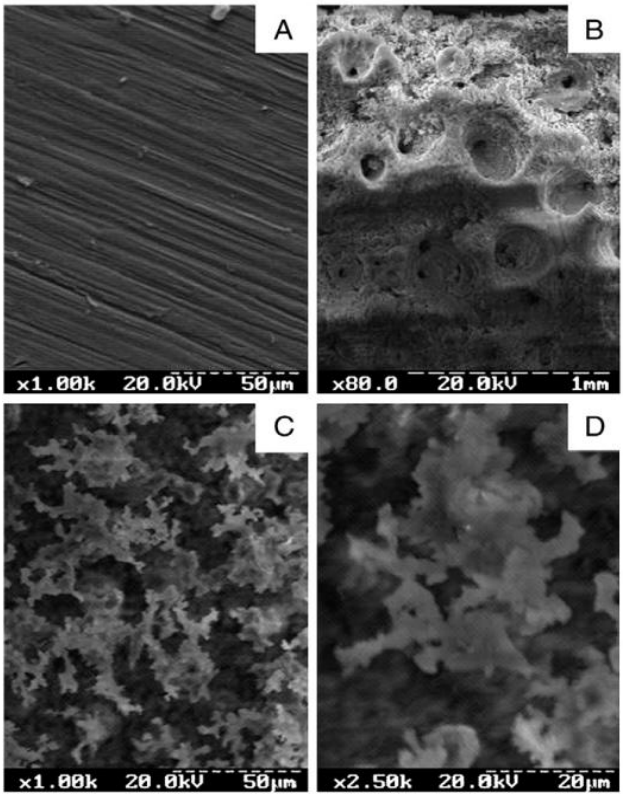

Fig. 11 – SEM micrographs showing the morphologies of (A) treated by NaOH surface and (B) HAp coating after deposition from the aqueous precursor solution by thermal substrate method. (C, D) are a higher magnification of (B). Copied from [29] with permission of Elsevier

the Ti6Al4V substrate TiO_2 is formed. Negatively charged Ti–O–groups interact with positively charged Ca^{2+} ions, which in turn attract phosphate ions from the precursor solution with formation of initial calcium-phosphate layer. Porous (pore diameter is nearly 150-200 μm) and thick HAp coating (1.04 mm) is formed on NaOH-modified surface (Fig. 11) [29]. H_2O_2-modified substrate was prepared by immersing the Ti-6Al-4V substrate in 200 ml of a 35 % H_2O_2 solution at 60 °C for 2 hours and than keeping at room temperature for 48 hours. The HAp coating was deposited by thermal substrate method under following conditions: substrate temperature of 105 °C, solution pH = 6.5, 2-hour treatment. Obtained porous HAp coating with pore sizes 100-150 μm (Fig. 12) [29]. The rough surface is formed on the substrate after its modification with

10 % HF solution (Fig. 13A). The phase composition of obtained coatings is presented in the Fig. 14.

New trend in a reparative surgery of bones *in situ* is connected with bone tissue engineering. This approach suggests that an organism able to reconstruct bone tissues if there are certain conditions. Many polymers able to biodegrade are applied in bone tissue

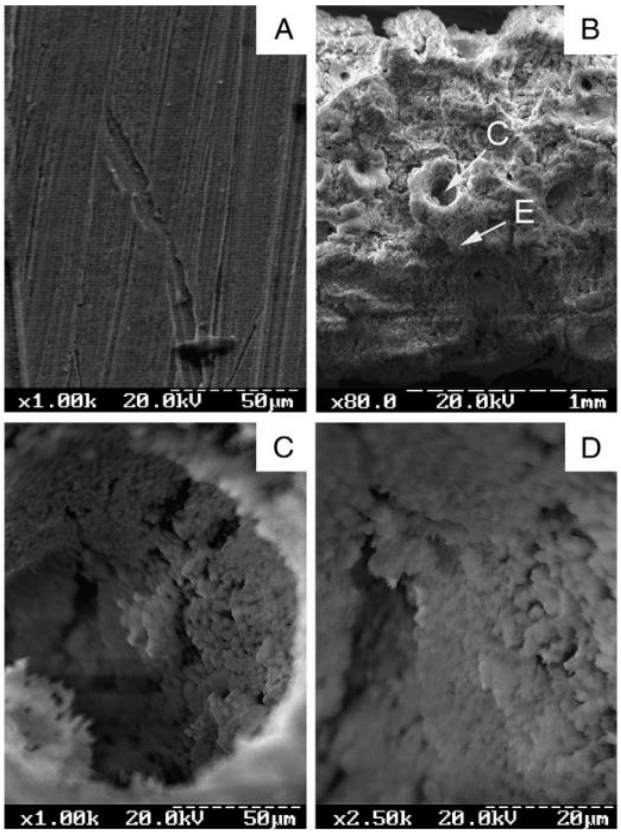

Fig. 12 – SEM images showing the morphologies of (A) H_2O_2-treated Ti-6Al-4V substrate; (B) H_2O_2-treated Ti-6Al-4V substrate after deposition of the HAp coating by thermal substrate method; (C, D) higher magnification of (B) in a pore. Copied from [29] with permission of Elsevier

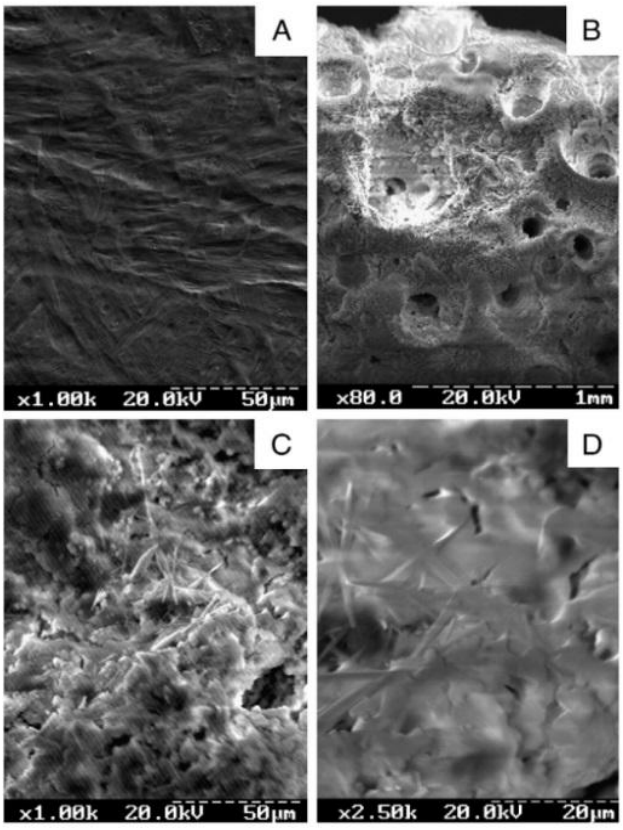

Fig. 13 – SEM images showing the morphologies of (A) HF-treated surface of the Ti-6Al-4V substrate; (B) HF-treated Ti-6Al-4V substrate after deposition of the HAp coating by thermal substrate method; (C, D) higher magnifications of (B). Copied from [29] with permission of Elsevier

engineering as a matrix [48]. Among synthetic polymers are the following: polyethylene glycol, polyvinyl alcohol, polyurethane. Natural polymers are of most interest due to their biological and chemical similarity to the tissues of an organism. Among them are alginates, gelatin, collagen, starch, chitosan [48]. The coatings formed with the thermal substrate method may be introduced with antibacterial and organic components (collagen, chitosan, gelatin and alginate). Collagen belongs to proteins of extra-cellular matrix. It consists of three polypeptide chains (α-chains) that form a structure of triplex. In animal tissues more than 27 collagen forms are present. Some of them (of I, II, III, V and XI type) are located in fibrils.

Collagen fibrils are characterized by a 67-nm axial periodicity; they also define the shape of the tissues in which they occur. Fibrils are arranged in complex three-dimensional arrays such as orthogonal lattices (e.g., in the cornea), parallel bundles (e.g., in ligament and tendon), and concentric weaves (e.g., in bone). They are characterized by three interwoven chains (a-chains) that can be homotrimeric or heterotrimeric, depending on the collagen type. The tight triple helix configuration is allowed by the repetitive Gly-X-Y triplet, where X can be any other amino acid, but is usually a proline, and Y is often a hydroxyproline. Glycine is an absolute requirement in every third position because it is the smallest amino acid that can occupy the limited space in the center of the triple helix [49].

Alginic acid is a linear polymer based on two monomeric units, b- D-mannuronic acid and a- L-guluronic acid. The alginate polymer is formed by joining these monomers at the C-1 and C-4 positions. An ether-oxygen bridge joins the carbon at the 1-position in one molecule to the 4-position of another molecule. It has been shown that the polymer chain is made up of three kinds of regions or blocks. The G blocks contain only units derived from L-guluronic acid, the M blocks are based entirely on D-mannuronic acid and the MG blocks consist of alternating units from D-mannuronic acid and L-guluronic acid [50]. *Chitosan* (CS) is a polysaccharide with a structure similar to cellulose. The pure compound is the polymer form of 2-amino-2-deoxy-D-glucopyranose with a 1-4-β-glucosidic bonding. The most important features of chitosan are its biodegradability, flexibility and high ability of forming intramolecular hydrogen bonds between hydroxyl and amino groups. It is one of the most promising biopolymers for possible orthopedic applications due to its fiber- and film-forming capacities, antibacterial activity, biocompatibility, biodegradation

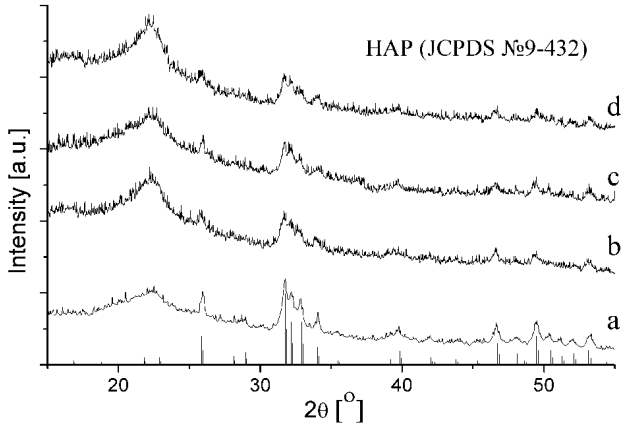

Fig. 14 – XRD diffraction patterns of coatings deposited from the precursor solution, containing Ca^{2+} and PO_4^{3-} ions. The HAp coating obtained by thermal substrate method at $T = 105$ °C, pH = 6.5, for 2 hours on the a) untreated Ti-6Al-4V substrate; b) NaOH-treated surface; c) HF-treated surface; and d) H_2O_2-treated surface. Copied from [29] with permission of Elsevier

capability, capability to form structures with predicted volume of pores. Thus chitosan is reasonable to be introduced into composite coatings in combination with hydroxyapatite. Variation of chitosan and hydroxyapatite concentrations allows obtaining coatings of various morphology, porosity, and crystallinity. Sequence of chitosan introduction is also of importance at coating formation by thermal substrate method: 1) chitosan film formation on a titanium substrate with further HAp deposition; 2) co-deposition of chitosan and HAp from aqueous solutions with various chitosan concentration; 3) HAp coating deposition with further immersion into a chitosan solution. The most appropriate is a co-deposition from aqueous solutions. The thermal substrate method allows combining optimum conditions of calcium-phosphate crystallization and chitosan existence in soluble form.

Apatite-biopolymer composite coatings. The initial solution for coating deposition was prepared by mixing solution containing $CaCl_2$ (10 mmol/dm^3) and NaH_2PO_4 (6 mmol/dm^3) in Ca / P relation 1.67. Chitosan solution (1 g/l) was prepared by dissolution of chitosan with molecular weight 200 kDa in 1 % acetic acid. Biomedical grade chitosan for experiments was supplied by the Haidebei Marine Bio Ltd. (Jinan, China) with 91 % degree of the deacetylation. When chitosan is dissolved into a diluted organic acid solution, its free amino groups are protonated and it transforms into a poly cation.. Solutions with various chitosan concentrations were prepared by dissolving the 1 g of chitosan fibers in 1 liter of 1 % CH_3COOH solution with vigorous stirring. In the same way the solution with chitosan concentration of 5 g/l was prepared. Chitosan solution with concentration of 1 g/l was diluted to the required CS concentrations: 0.025; 0.05; 0.1 g/l by mixing with the initial solution for HAp synthesis containing $CaCl_2$ (10 mmol/l) and NaH_2PO_4 (6 mmol/l). For film formation Ti-6Al-4V alloy was immersed into solution having chitosan concentration of 5 g/l followed by immersion into 10 M NaOH solution. Chitosan films were dried in the air for 24 hours. Hydroxyapatite coatings were deposited on the Ti–6Al–4V substrates modified with chitosan films by TSM method under following conditions: substrate temperature 80 °C, pH of the initial solution 6.65-6.72, deposition time – 60 min. Chitosan films create an interface between titanium substrate and hydroxyapatite coatings deposited by thermal substrate method. After immersion in the initial solution containing $CaCl_2$ and NaH_2PO_4 in such concentrations that Ca / P relation is 1.67 (as described above) at pH = 6.5-7.0, NH_2-groups of chitosan create crystallization centers on the substrate surface which promote HAp crystallization. It is an acceptable way of chitosan insertion into HAp coatings deposited by the thermal substrate method. Hydroxyapatite coatings with further immersion into a chitosan solution (at pH = 6.5) for twenty four hours are less effective since a partial dissolution of a coatings take place there. The perspective way of chitosan doping into hydroxyapatite coatings is co-deposition by TSM from aqueous solutions having various CS concentrations: 0.1 g/l (a), 0.05 g/l (b) and 0.025 g/l (c) and mentioned components for apatite synthesis. Coatings were deposited under following conditions: substrate temperature 80 °C, pH of the initial solution 6.65, deposition time – 60 min. An inorganic phase of the coating is HAp, an organic one corresponds to chitosan (Fig. 15). Received coatings differ greatly in their morphology. Due to their organic component the coating have a porous structure. Through variation of chitosan concentration in the initial solution it is possible to vary porosity, coating density and morphology. If chitosan concentration decreases in the initial solution the pores become less deep and the whole coating is more uniform (Fig. 15).

The variation in coatings morphology is observed depending on the initial CS concentration in the solution. For coatings obtained from solutions having CS concentration of 0.025 g/L a homogeneous surface morphology is observed. The intensities of HAp peaks are significantly higher for coatings having lower chitosan concentrations (Fig. 15) which can be explained by higher HAp crystallinity. This may be related to chitosan macromolecules binding with components in the initial solution and prevent a common process of crystallization. Interaction of inorganic crystals and organic molecules in this case is the beginning of crystallization process. Precipitation depends on a type and concentration of substances added to the solution. Hydroxyapatite nucleation started by adsorption of chitosan at the surface of nuclei, an interfacial energy decreases and the rate of crystal nucleation increases. Organic molecules may occupy places of growth on crystal nuclei and limit growth of grains, therefore, the crystal growth may be reduced by a polymer adsorption. Morphology and composition of deposits could be changed according to described effects. Adsorption of chitosan molecules on crystal surfaces reduces the interfacial energy at the"crystal / solution" interface and the surface cannot promote precipitation of the Ca^{2+} and PO_4^{3-} ions that may precipitate only on nuclei vacant from the polymer molecules. Chitosan as a polyelectrolyte may induce aggregation at low concentrations via binding the particles distributed into suspensions. In its greater concentration chitosan may act as a stabilizing component and its adsorption creates a charge. Introduction of chitosan molecules into calcium-phosphate coatings at co-deposition using thermal

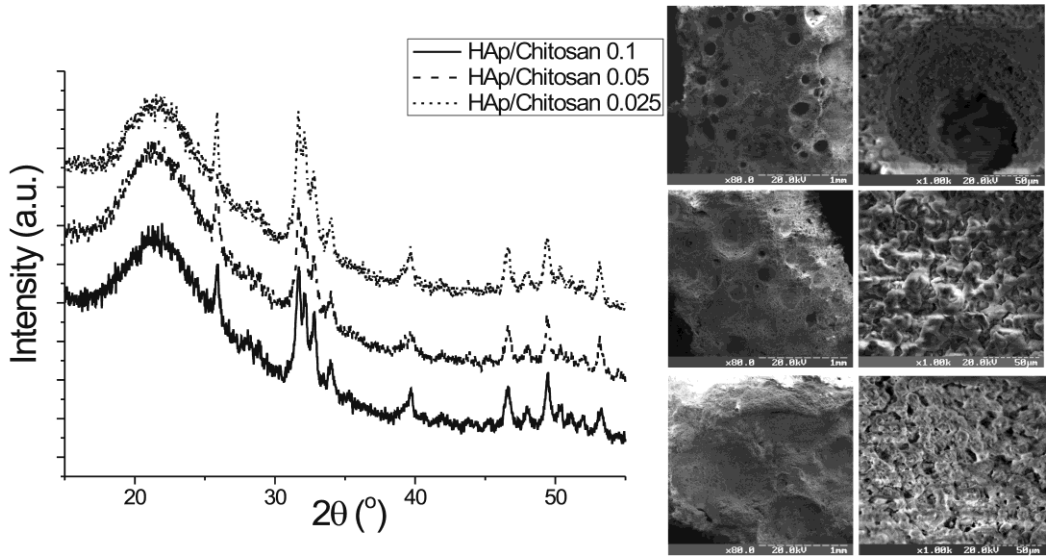

Fig. 15 – Morphology and phase composition of the HAp-CS coatings co-deposited by TSM method from aqueous solutions having chitosan concentrations (from top to bottom) of 0.1 g/l, 0.05 g/l, 0.025 g/l.

substrate method allows enhancing biocompatibility and osteointegration of implants without considerable changes in Ca / P ratio that is typical for a bone tissue.

4. CONCLUSIONS

The results of the studies, conducted at the recently created Sumy state university "Bionanocomposite" laboratory, of nanomaterials mainly based on calcium phosphates and natural polymers, are shown in this short review. The crystallite sizes of the studied materials, which were synthesized primarily chemically, vary from 25 to 75 nm.

Objects with their sizes span within this range at least in the single dimension are called nanomaterials according to International Organization for Standardization (IOS) definition. Such a demand is specified because such crystallite size is its most important advantage over macroobjects, since it is connected with their specific properties: large surface square, transfer of bioactive substances to the substrate with their further release for a specified time, their action locality and cell interaction specificity [51].

The two major groups of nanoparticles (NP) are formed according to their nature: organic and inorganic one. Liposomes, lipids, polymers and protein nanostructures are referred to the organic NPs. Calcium phosphorous NPs (CaPNPs) attract most attention from the inorganic NPs to which, e.g., nanosized gold, silver, quartz nanoparticles, iron oxides, quantum dots, carbon nanowires are also referred. CaPNPs are characterized with high biocompatibility, low toxicity, stability, and that is why are used together with quantum dots and gold NPs in the diagnostics of different diseases, specifically, cancer, by the visualization of tumor deposits.

In addition, the gene level therapy seems perspective: the transfection of DNA, RNA in eukaryotic cells both in the nucleus and mitochondrion, and also the use of CaPNPs for drug delivery, imaging, vaccination and local healing of tissue (tumor thermotherapy) [52].

The microoverview paper describes synthesis and characterization of novel third generation composite biomaterials and coatings which correspond to the second structural level of human bone tissue (HBT) organization obtained at Sumy state university "Bionanocomposite" laboratory. To obtain such composites an animal collagen is usually used, which is not potentially safe for medical applications. That is why investigations were started using some other biopolymers to obtain composites close to the second level in the structural hierarchy of HBT. Proposed natural polymers (Na alginate, chitosan) are the most perspective because they have bacteriostatic properties for a vast number of aerobic and anaerobic bacteria, high biocompatibility towards the connective tissue, low toxicity, an ability to improve regenerative processes during wounds healing, degradation ability with the creation of chemotaxic activity towards fibroblasts and osteoblasts. The formation of nanosized (25-75 nm) calcium deficient hydroxyapatite (cdHA) particles in the polymer scaffold approaches the derived material to the biogenic bone tissue, which can provide its more effective implantation.

The influence of the imposition of static magnetic field on brushite ($CaHPO_4 \cdot 2H_2O$) crystallization was also investigated. It was shown that changing the magnetic field configuration could greatly affect their crystallinity and texture with most of them having the preferred orientation along the b-axis.

To increase the biocompatibility of existing medical implants (Ti 6Al 4V, Ti Ni, Mg) the technology for obtaining bioactive coatings with corresponding mechanical, structural and morphology characteristics is developed in our laboratory. In this direction coatings based on cdHA in combination with biopolymer matrices (Na alginate, chitosan) are obtained in "soft" conditions using a thermal substrate technology. This technology was proposed by Japan scientists [1] and was sufficiently improved by us [2] in order to obtain coatings in the controlled mode.

ACKNOWLEDGEMENTS

We thank the Ukrainian Fundamental Foundation (project NU/7-2013) for funding our researches, Dr. V.G. Lugin from State technological university of Belarus for IR- and EM-studies of some of our apatite-biopolymer samples.

Нанокомпозитные апатит-биополимерные материалы и покрытия для биомедицинского применения

Л.Ф. Суходуб[1], А.А. Яновская[2], Л.Б. Суходуб[1], В.Н. Кузнецов[2], А.С. Станиславов[2]

[1] *Сумский государственный университет министерства образования и науки Украины, ул. Римского-Корсакова, 2, 40007 Сумы, Украина*
[2] *Институт прикладной физики Национальной академии наук Украины, ул. Петропавловская, 58, 40007 Сумы, Украина*

В данном обзоре описываются синтез и свойства новейших композитных биоматериалов и покрытий третьего поколения, относящихся ко второму структурному уровню организации костной ткани человека (КТЧ). Для получения подобных композитов обычно используется животный коллаген, который является потенциально опасным для медицинского применения, поэтому нами были начаты исследования с использованием других биополимеров для получения композитов, близких ко второму уровню структурной иерархии КТЧ.

Предложенные природные полимеры (альгинат натрия, хитозан) являются наиболее перспективными, поскольку они обладают бактериостатичными свойствами для огромного количества аэробных и анаэробных бактерий, высокой биосовместимостью по отношению к соединительной ткани, низкой токсичностью, возможностью ускорять восстановительные процессы во время лечения ран, свойством деградации с созданием хемотаксисной активности по отношению к фибробластам и остеобластам. Формирование наноразмерных (25-75 нм) частичек кальцийдефицитного гидроксиапатита (КДГА) в полимерном скаффолде приближает полученные материалы к КТЧ, что, в свою очередь, способствует их более эффективной имплантации.

Также было изучено влияние статического магнитного поля на кристаллизацию брушита ($CaHPO_4{\cdot}2H_2O$). Показано, что изменение конфигурации магнитного поля оказывает значительное влияние на кристалличность и текстуру полученных частичек.

Для улучшения биосовместимости существующих медицинских имплантатов (Ti–6Al–4V, Ti–Ni, Mg) в нашей лаборатории была усовершенствована [2] предложенная японскими учеными [1] технология получения биоактивных покрытий с соответствующими механическими, структурными и морфологическими характеристиками. Покрытия на основе КДГА в сочетании с биополимерной матрицей (альгинат Na, хитозан) синтезируются методом термодепозиции в «мягких» условиях.

Ключевые слова: Композитные биоматериалы, Гидроксиапатит, Покрытия, Хитозан, Альгинат, рентгеновская дифракция, рентгенфлуоресцентный анализ, ИК спектроскопия с преобразованием Фурье, ПЭМ, РЭМ.

Нанокомпозитні апатит-біополімерні матеріали та покриття для біомедичного застосування

Л.Ф. Суходуб[1], Г.О. Яновська[2], Л.Б. Суходуб[1], В.М. Кузнецов[2], О.С. Станіславов[2]

[1] *Сумський державний університет Міністерства освіти та науки України, вул. Римського-Корсакова, 2, 40007 Суми, Україна*
[2] *Інститут прикладної фізики Національної академії наук України, вул. Петропавлівська, 58, 40007 Суми, Україна*

В даному огляді описуються синтез та властивості новітніх композитних біоматеріалів та покриттів третього покоління, що відносяться до другого структурного рівня організації кісткової тканини людини (КТЛ). Для отримання подібних композитів за звичай застосовується тваринний колаген, котрий є потенційно небезпечним у медичному застосуванні, тому нами були розпочати дослідження з застосуванням інших біополімерів для отримання композитів, близьких до другого рівня структурної ієрархії КТЛ.

Запропоновані природні полімери (альгінат натрію, хітозан) є найбільш перспективними, оскільки вони мають бактеріостатичні властивості для великої кількості аеробних та анаеробних бактерій, високою біосумісністю по відношенню до з'єднувальної тканини, низькою токсичністю, можливістю прискорювати регенеративні процеси під час лікування ран, здібністю деградації зі створенням хемотаксисної активності по відношенню до фібробластів та остеобластів. Формування нанорозмірних (25-75 нм) частинок кальційдефіцитного гідроксиапатиту (КДГА) у полімерному скафолді наближує отримані матеріали до КТЛ, що, в свою чергу, сприяє їх більш ефективній імплантації.

Також було досліджено вплив статичного магнітного поля на кристалізацію брушиту ($CaHPO_4{\cdot}2H_2O$). Зміна конфігурації магнітного поля оказує суттєвий вплив на кристалічність та текстуру отриманих частинок.

Для покращення біосумісності існуючих медичних імплантатів (Ti-6Al-4V, Ti-Ni, Mg) в нашій лабораторії була вдосконалена [2] запропонована японськими вченими [1] технологія отримання біоактивних покриттів з відповідними механічними, структурними та морфологічними характеристиками. Покриття на базі КДГА в поєднанні з біополімерною матрицею (альгінат Na, хітозан) синтезуються методом термодепозиції в «м'яких» умовах.

Ключові слова: Композитні біоматеріали, Гідроксиапатит, Покриття, Хітозан, Альгінат, рентгенівська дифракція, рентгенфлуоресцентний аналіз, ІЧ спектроскопія з перетворенням Фур'є, ПЕМ, РЕМ.

REFERENCES

1. M. Okido, K. Kuroda, M. Ishikawa, R. Ichino, O. Takai, *Solid State Ionics* **151**, 47 (2002).
2. L.B. Sukhodub, C. Moseke, L.F. Sukhodub, V.V. Pilipenko, B. Sulkio-Cleff, *Annual Report* 86 (2002/2003).
3. T. Kanazawa, *Inorganic phosphate materials* (Amsterdam: Elsevier Science: 2005).
4. M. Bohner, U. Gbureck, J.E. Barralet, *Biomaterials* **26**, 6423 (2005).
5. M. Kumar, H. Dasarathy, C. Riley, *J. Biomed. Mater. Res.* **45**, 302 (1999).
6. D. Lee, P.N. Kumta, *Mater. Sci. Eng.: C* **30**, 934 (2010).
7. J.C. Elliott, *Structure and Chemistry of the Apatites and Other Calcium Orthophosphates* (London: Elsevier: 1994).
8. G. Wang, H. Zreiqat, *Materials* **3**, 3994 (2010).
9. B. León, J.A. Jansen, *Thin Calcium Phosphate Coatings for Medical Implants* (Berlin: Springer: 2009).
10. X. Zheng, M. Huang, C. Ding, *Biomaterials* **21**, 841 (2000).
11. Y. Yang, K.-H. Kimc, J.L. Ong, *Biomaterials* **26**, 327 (2005).
12. V.F. Pichugina, R.A. Surmeneva, E.V. Shesterikova, M.A. Ryabtsevaa, E.V. Eshenkoa, S.I. Tverdokhlebova, O. Prymakb, M. Epple, *Surf. Coat. Tech.* **202**, 3913 (2008).
13. A.R. Boyd, H. Duffy, R. McCann, B.J. Meenan, *Mater. Sci. Eng.: C* **28,** 228 (2008).
14. J.G. Wolke, J.P. van der Waerden, H.G. Schaeken, J.A. Jansen, *Biomaterials* **24**, 2623 (2003).
15. L.F. Sukhodub, C. Moseke, A.B. Brik, O. Boeling, B. Sulkio-Cleff, *Mineral. J.* **23**, 65 (2001).
16. H. Zeng, W.R. Lacefield, *Biomaterials* **21**, 23 (2000).
17. M. Yoshinari, K. Ozeki, T. Sumii, *Bull. Tokyo Dent. Coll.* **32**, 147 (1991).
18. M.T. Pham, H. Reuther, W. Matz, R. Mueller, G. Steiner, S. Oswald, I. Zyganov, *J. Mater. Sci. Mater. Med.* **11**, 383 (2000).
19. W. Weng, S. Zhangb, K. Chenga, H. Qua, P. Dua, G. Shena, J. Yuana, G. Han, *Surf. Coat. Tech.* **167**, 292 (2003).
20. U. Vijayalakshmi, S. Rajeswari, *Trends Biomater. Artif. Organs* **19** (2), 57 (2006).
21. Y. Han, T. Fu, J. Lu, K. Xu, *J. Biomed. Mater. Res.* **54** (1), 96 (2001).
22. M. Manso, C. Jiménez, C. Morant, P. Herrerob, J.M. Martinez-Duarta, *Biomaterials* **21**, 1755 (2000).
23. J. Wang, J. de Boer, K. de Groot, *J. Dent. Res.* **83**, 296 (2004).
24. S.C.G. Leeuwenburgh, J.G.C. Wolke, L. Lommen, T. Pooters, J. Schoonman, J.A. Jansen, *J. Biomed. Mater. Res. A.* **78A** (3), 558 (2006).
25. T.V. Thamaraiselvi, K. Prabakaran, S. Rajeswari, *Trends Biomater. Artif. Organs* **19** (2), 81 (2006).
26. K. Kuroda, R. Ichino, M. Okido, O. Takai, *J. Biomed. Mat. Res.* **61**, 354 (2002).
27. M. Okido, K. Kuroda, R. Ichino, *Mater. Sci. Forum* **426-432**, 3457 (2003).
28. K. Kuroda, Y. Miyashita, R. Ichino, M. Okido, O. Takai, *Mater. Trans.* **43**, 3015 (2002).
29. A. Yanovska, V. Kuznetsov, A. Stanislavov, S. Danilchenko, L. Sukhodub, *J. Surf. Coat. Tech.* **205**, 5324 (2011).
30. H.P. Klug, L.E. Alexander, *X-Ray Diffraction Procedures: For Polycrystalline and Amorphous Materials* (New York: Wiley: 1974).
31. F.H. Chung, *J. Appl. Crystallogr.* **8**, 17 (1975).
32. S. Raynaud, E. Champion, D. Bernache-Assollant, J.-P. Laval, *J. Am. Ceram. Soc.* **84** No2, 359 (2001).
33. L.B. Sukhodub, V.N. Kuznetsov, A.S. Stanislavov, N.N. Inshina, A.I. Kulak, L.F. Sukhodub, *Proc. Intern. Conf. NAP* **2**, No4, 04NABM15 (2013).
34. A. Yanovska, V. Kuznetsov, A. Stanislavov, S. Danilchenko, L. Sukhodub, *Mater. Sci. Eng.: C* **32**, 1883 (2012).
35. K. Kuroda, S. Nakamoto, Y. Miyashita, R. Ichino, M. Okido, *Mater. Trans.* **47** (5), 1391 (2006).
36. A.A. Yanovska, V.N. Kuznetsov, S.N. Danilchenko, L.F. Sukhodub, *Biophysical Bulletin* **25** (2), 131 (2010).
37. K. Kuroda, S. Nakamoto, R. Ichino, M. Okido, R.M. Pilliar, *Mater. Trans.* **46** (7), 1633 (2005).
38. K. Kuroda, Y. Miyashita, R. Ichino, M. Okido, O. Takai, *Mater. Trans.* **47** (5), 1391 (2006).
39. K. Kuroda, M. Okido, *Bioinorg. Chem. Appl.* **2012**, 730693 (2012).
40. M. Ueda, T. Kinoshita, M. Ikeda, M. Ogawa, *Mat. Sci. Eng.:C* **29**, 2246 (2009).
41. N. Chosa, M. Taira, S. Saitoh, N. Sato, Y. Araki, *J. Dent. Res.* **83**, 465 (2004).
42. J.-H. Park, D.-Y. Lee, K.-T. Oh, Y.-K. Lee, K.-N. Kim, *J. Am. Ceram. Soc.* **87**, 1792 (2004).
43. Y.K. Lee, K.M. Kim, K.N. Kim, *J. Surf. Coat. Tech.* **195**, 252 (2005).
44. J.P. Bearinger, C.A. Orme, J.L. Gilbert, *J. Biomed. Mater. Res. A.* **67**, 702 (2003).
45. D. Horkavcová, I. Štěpánek, B. Plešingerová, *Acta Metall. Slovaca* **15** (1), 37 (2009).
46. D. Lakstein, W. Kopelovitch, Z. Barkay, M. Bahaad, D. Hendelb, N. Eliaz, *Acta Biomater.* **5**, 2258 (2009).
47. N. Eliaz, S. Shmueli, I. Shur, D. Benayahu, D. Aronov, G. Rosenman, *Acta Biomater.* **5**, 3178 (2009).
48. I.-Y. Kim, S.-J. Seo, H.-S. Moon, M.-K. Yoo, I.-Y. Park, B.-C. Kim, C.-S. Cho, *Biotechnol. Adv.* **26**, 1 (2008).
49. S. Viguet-Carrin, P. Garnero, P.D. Delmas, *Osteoporosis Int.* **17**, 319 (2006).
50. H. Grasdalen, B. Larsen, O. Smidsrod, *Carbohydt. Res.* **89**, 179 (1981).
51. S. Chornousova, M. Epple, *Nanosystems, Nanomaterials, Nanotechnologies* **10** (4), 667 (2012).
52. D. Kozlova, M. Epple, *BioNanoMaterials* **14** (3-4), 161 (2013).